

Role of Cyclooxygenase-2 Pathway in Creating an Immunosuppressive Microenvironment and in Initiation and Progression of Wilms' Tumor



Paramahansa Maturu^{*,†}, Devin Jones^{*},
E. Cristy Ruteshouser^{*}, Qianghua Hu^{*},
Joseph M Reynolds[‡], John Hicks[§], Nagireddy Putluri[¶],
Suhendan Ekmekcioglu^{†,||}, Elizabeth A. Grimm^{†,||},
Chen Dong[‡] and Willem W Overwijk^{||}

^{*}Department of Genetics, The University of Texas MD Anderson Cancer Center, 1515 Holcombe Blvd, Unit 1010, Houston, TX 77030, USA; [†]Department of Pediatrics, Section of Neonatology, Texas Children's Hospital, Baylor College of Medicine, Houston, TX 77030, USA; [‡]Department of Immunology and Center for Inflammation and Cancer, The University of Texas MD Anderson Cancer Center, Houston, Texas, USA; [§]Department of Pathology, Texas Children's Hospital, 6621 Fannin, Houston, TX, USA; [¶]Department of Molecular and Cellular Biology, Baylor College of Medicine, Houston, TX, USA; ^{||}Department of Melanoma Cancer Medical Oncology, The University of Texas MD Anderson Cancer Center, 1515 Holcombe Blvd, Unit 0904, Houston, TX, USA

Abstract

Wilms' tumors (WT), which account for 6% of all childhood cancers, arise from dysregulated differentiation of nephrogenic progenitor cells from embryonic kidneys. Though there is an improvement in the prognosis of WT, still 10% of patients with WT die due to recurrence. Thus more effective treatment approaches are necessary. We previously characterized the inflammatory microenvironment in human WT and observed the robust expression of COX-2. The aim of this study was to extend our studies to analyze the role of COX-2 pathway components in WT progression using a mouse model of WT. Herein, COX-2 pathway components such as COX-2, HIF-1 α , p-ERK1/2, and p-STAT3 were upregulated in mouse and human tumor tissues. In our RPPA analysis, COX-2 was up-regulated in M15 cells after Wt1 gene was knocked down. Flow cytometry analysis showed the increased infiltration of immune suppressive inflammatory cells such as pDCs and Treg cells in tumors. The chemotactic chemokines responsible for the infiltration of these cells were also induced in CCR5 and CXCR4 dependent manner respectively. The immunosuppressive cytokines IL-10, TGF- β , and TNF- α were also up-regulated. Furthermore, more pronounced Th2 and Treg induced cytokine response was observed than Th1 response in tumors. Basing on all these evidences it is speculated that COX-2 pathway may be a beneficial target for the treatment of WT. It may be most effective as an adjuvant therapy together with other inhibitors. Thus, our current study provides a good rationale for initiating animal studies to confirm the efficacy of COX-2 inhibitors in decreasing tumor cell growth in vivo.

Neoplasia (2017) 19, 237–249

Introduction

Wilms' tumor (WT), a pediatric tumor of the kidney, is the second most common cancer of children, accounting for approximately 6% of all childhood cancers [1]. While there has been slight improvement in the prognosis of WT in recent years, 10% of patients with WT still experience disease recurrence, and many of those die of their disease. Thus, the development of new, more effective approaches to treat this lethal malignancy is of considerable interest. Though mutations in WT1 and β -catenin are known to be involved in Wilms'

Abbreviations: WT, Wilms' tumor; COX-2, Cyclooxygenase-2; *Wt1*, Wilms' Tumor 1 gene; Igf2, Insulin Growth Factor2; HIF-1 α , Hypoxia-inducible factor 1-alpha; IDO, Indolamine 2, 3-dioxygenase; TGF- β , Transforming growth factor beta; TNF- α , Tumor necrosis factor alpha; pDCs, Plasmacytoid Dendritic Cells; Tregs, T regulatory Cells; RPPA, Reverse Phase Protein Array
Address all correspondence to Dr. Paramahansa Maturu, Department of Pediatrics, Section of Neonatology, Texas Children's Hospital, Baylor College of Medicine, 1102 Bates Avenue, MC: FC510, Houston, TX 77030, USA. Tel. +1 832-824-3225; Fax: +1 832-824-3204.

E-mail: maturu@bcm.edu

Received 13 April 2016; Revised 19 July 2016; Accepted 21 July 2016

© 2016 The Authors. Published by Elsevier Inc. on behalf of Neoplasia Press, Inc. This is an open access article under the CC BY-NC-ND license (<http://creativecommons.org/licenses/by-nc-nd/4.0/>).
1476-5586

<http://dx.doi.org/10.1016/j.neo.2016.07.009>

tumorigenesis [2], the exact molecular pathogenesis of this cancer is unclear. Elucidation of these mechanisms will substantially improve our understanding of the pathways involved in WT tumorigenesis and aid in the development of more effective therapies.

There has been increasing awareness and emphasis on the role of the tumor microenvironment in tumorigenesis and, potentially in cancer therapy. It is now believed that characterizing the components within the tumor microenvironment that are involved in tumor growth and progression and the pathways that regulate them will lead to identification of novel prognostic markers and tumor-associated therapeutic targets. Though the relationship between chronic inflammation and cancer and the components of inflammation that are responsible for tumor development have been reported in various cancers, no information is available on the role of these critical components in WT development. To do this, we previously defined and characterized the inflammatory microenvironment in human WT where we have observed the robust expression of inflammatory marker Cyclooxygenase-2 (COX-2) [3] in almost all the tumors we have analyzed (3). Our purpose in the current study is to extend those studies to analyze the contribution of the microenvironment in particular, the role of COX-2 and its pathway components in WT progression using a mouse model of Wilms' tumor in detail. We thus characterized the tumor microenvironment in a mouse model of WT that was generated in our laboratory by *Wt1* ablation and *Igf2* up regulation [4]. In these mouse tumors and in littermate control kidney tissues, we evaluated and defined the expression of various inflammatory markers by immunohistochemical (IHC) analysis; isolated and identified the inflammatory cells regulated by the cyclooxygenase-2 (COX-2) pathway by flow cytometry; and quantified expression of various inflammatory chemokines, chemokine receptors, and inflammatory cytokines by quantitative polymerase chain reaction (qPCR) and other methods. Our results indicated that the WT tumor microenvironment is enriched with immunosuppressive inflammatory cells, trafficking of which is regulated by COX-2. The important role of these inflammatory cells in creating immunosuppressive tumor microenvironment and the role of COX-2 in immunosuppressive immune cell production and trafficking are also elucidated. This new understanding of the mechanisms underlying WT progression will be useful in planning for the use of specific inhibitors to treat these tumors.

Materials and Methods

Animal Experiments

All animal experiments were approved by the Institutional Animal Care and Use committee of The University of Texas MD Anderson Cancer Center. *Wt1* was inactivated mosaically or almost completely in *Wt1*-*flCre-ER* embryos by in utero treatment of pregnant mice with tamoxifen (1 mg/40 g body weight) at E11.5. This treatment resulted in Cre-recombinase activity in approximately 5–10% of cells. All embryos carried a maternally inherited *H19*⁻ allele that results in up regulation of *Igf2* as a result of loss of imprinting and biallelic expression of *Igf2*.

Human Tissue Samples

Human WT tissues and autologous normal kidney specimens were obtained from 16 WT patients aged 7 to 66 months at the time of diagnosis. Eight of the patients were males and eight were females, and one patient had bilateral disease. Of these 16 patients, 4 were at stage IV, 4 were at stage III, 3 were at stage II, and 5 were

at stage I of WT disease. Informed consent was obtained from each patient's parent or guardian. Studies were approved by the Institutional Review Board and in accordance with an assurance filed with and approved by the US Department of Health and Human Services.

Immunohistochemical Analysis of Inflammatory Markers

Tissue processing. Tumor tissues and control kidney samples were collected from mice and fixed in 10% neutral-buffered formalin. After 12–16 hours, formalin was replaced with 70% ethanol; the samples were subjected to dehydration by a series of graded alcohols and xylene and then embedded in paraffin. The tissues were then cut in 5- μ m sections using a Leica 2135 microtome.

Analysis. Sections were deparaffinized and used for Hematoxylin and Eosin staining and IHC analysis of various markers. The paraffin-embedded tissue sections from mice and humans were deparaffinized in xylene, rehydrated sequentially in a graded series of ethanol's (100, 90, and 70%), and placed into 1% phosphate-buffered saline solution (PBS; pH 7.4). The epitope retrieval was performed by heating for 45 minutes in 1 mM Tris EDTA pH 9.0 buffer in a water bath at 95–100°C for COX-2 and hypoxia-inducible factor 1- α (HIF-1 α), in 10 mM Tris+ 0.5 mM EGTA pH 9.0 buffer for phospho-ERK1/2, and in 1 mM EDTA pH 9.0 buffer for p-STAT3. The sections were cooled at room temperature in the buffer for 1 hour, washed three times with 1 \times PBS for 5 minutes/wash, and incubated with 10% normal serum to block nonspecific protein binding. Expression of inflammatory markers was detected by applying the following antibodies: polyclonal goat anti-mouse/human COX-2, 1:100 dilution (Santa Cruz Biotechnology SC-1747); polyclonal rabbit anti-mouse/human HIF-1 α , 1:100 dilution (Novus Biologicals NB100-479); monoclonal rabbit anti-mouse/human phospho-p44/42 ERK1/2, 1:100 dilution (Cell Signaling Technology Cat #4376); and rabbit monoclonal anti-mouse/human phospho-STAT3 (Cell Signaling Technology Cat #9145); sections were incubated in 2.5% appropriate normal serum overnight at 4°C in a humidified chamber. The sections were then washed three times with 1 \times PBS (10 minutes/wash) and incubated with the appropriate secondary antibody IgG (H + L) solution (biotinylated goat anti-rat IgG 1:500, biotinylated goat anti-rabbit IgG 1:500, biotinylated goat anti-mouse IgG 1:500, or biotinylated rabbit anti-goat IgG 1:500, respectively) in 2.5% normal serum for 1 hour at room temperature. An optimized control-positive tissue section and a negative control section for endogenous staining by omission of the primary antibody were included with every immunostaining batch. The bound positive cells were detected by applying the Vectastain Elite ABC reagents (Vector Laboratories, Inc., Burlingame, CA) and avidin DH: biotinylated horseradish peroxidase H complex with 3, 3'-diaminobenzidine (Vector Laboratories, Inc.) and counterstaining with Mayer hematoxylin (Fisher Scientific, Fair Lawn, NJ). Images were captured by an Olympus BX60 microscope.

Flow Cytometry

Single cell preparation. To prepare single-cell suspensions from tumors and control kidneys for flow cytometry analysis, tumors and normal kidneys were cut, washed with RPMI medium to remove blood, and weighed. Tissues were minced and digested with 10 mL of digestion medium (Type IV Collagenase 1 mg/mL in RPMI 1640 medium) by incubating the fragments for 30 minutes [Sigma-Aldrich, St. Louis, MO] in 100-mL conical trypsinization flasks with tumor digestion media. During this incubation, the tissues were subjected to

continuous shaking with intermittent pipetting up and down and then were filtered through a 70- μ m nylon Falcon filter (BD Biosciences, San Jose, CA). The filtrates were subjected to centrifugation at 4°C at 1500 rpm for 5 minutes. Pellets were resuspended in ice-cold 1 \times PBS, and the resulting single-cell suspensions were treated with Pharm Lyse ammonium chloride lysing reagent (BD Biosciences) for less than a minute to remove erythrocytes. The pellet was resuspended in 5 mL of a solution of 0.1% fetal bovine serum (FBS) in 1 \times PBS and subjected to centrifugation at 1500 rpm for 5 minutes at 4°C, after which the supernatant was aspirated carefully without touching the pellet. Finally, the cells were resuspended in 5–10 mL of the 1 \times PBS+ 0.1% FBS medium and counted by using a hemocytometer; aliquots of approximately 1 million cells were stained for flow cytometry.

Reagents and antibodies. Monoclonal antibodies CD3e-ApcCy7, CD45-PerCPCy5.5, Gr1-APC, CD8-PECy7, CD25-FITC, CD11b-FITC, CD11c-PE, B220-PB, and NK1.1-PE were purchased from BD Biosciences. Foxp3-APC and F4/80-PE were purchased from eBioscience and CD4-PO and calcein violet from Invitrogen.

Analysis. A master mixture was prepared in two sets, each containing a mixture of different antibodies (Supplementary Table 1). All antibodies were prepared in 1:100 dilutions. The antibody mixtures were suspended in ice-cold 1 \times PBS with 1% bovine serum albumin (BSA). The master mix (100 μ L) was added to the prepared cells, which were incubated on ice for 1 hour with gentle shaking. The cells then were washed two or three times with ice-cold 1 \times PBS+ 1% BSA buffer and resuspended in 100 μ L of washing buffer. The antibody mixture also contained live and dead fixable aqua (Molecular Probes, Cat #L34957) to discriminate between viable and dead cells.

Flow cytometry data were acquired on a FACSCalibur using CellQuestPro software (BD Biosciences) and analyzed by using FlowJo software (Tree Star, Inc.). Gates were set by using negative controls, and positive populations were corrected by subtraction of background and nonspecific binding of the antibody.

T-helper cell (Th) response analysis. After single cell preparation from the tumor cells as well as control kidneys as described above, CD4 + T cells isolated and were differentiated into Th1, Th2, and Th17 lineages. For intracellular cytokine analysis, cells were restimulated with 500 ng/ml of ionomycin and 50 ng/ml of PMA in the presence of Golgi Stop (BD Pharmingen) for 5 hr. Cells were then permeabilized with Cytotfix/Cytoperm Kit (BD Pharmingen) and analyzed for the expression of IL-4, IL-5, IL-9, IL-13, IL-17A or IFN- γ (BD Pharmingen) by FACSCalibur analysis.

Cells. M15 mouse mesonephric cells which are known to express high amount of WT1 m-RNA as well as protein were maintained as previously described. [5].

siRNA knockdown of *Wt1*. Knockdown of *Wt1* in mouse mesenchymal cell line M15 was performed by transfection of scrambled *Wt1* siRNA (ON-TARGET plus SMARTpool duplex, Dharmacon) using media supplemented with 10 μ L of HyperFect Transfection Reagent (Qiagen). Cells were plated into 6 well plates at 8 \times 10⁴ cells per well and allowed to grow overnight before adding 50 nm siRNA. Following 24 hours of *Wt1* siRNA treatment, RNA and protein lysates were collected and analyzed.

Reverse-phase Protein Analysis

Selected cancer-related proteins were quantified by reverse-phase protein analysis (RPPA) in M15 cells treated with the siRNA for WT1 as previously described [6]. Briefly, protein extracts were

prepared from M15 cells with and without WT1 knockdown. Protein extracts were quantified, denatured, and subjected to 50- to 60-fold serial dilutions. The samples were then arrayed on multiple slides along with positive and negative controls prepared from mixed cell lysates or dilution buffer. Each slide was primary antibody validated with respect to specificity, reproducibility, high dynamic range of the assay, correlation with Western blotting data, etc., and with a biotin-conjugated secondary antibody. After staining, slides were scanned, and spot intensities were analyzed, quantified, and normalized. Heat maps were generated from log₂ median-centered data by the Cluster algorithm [7].

Quantitative Polymerase Chain Reaction Analysis of Inflammatory Cytokines

RNA preparation. RNA samples were prepared with the total-RNA Easy Mini Prep kit (Qiagen, Hilden, Germany) with a DNase step, according to the instructions of the manufacturer.

Real-time PCR. For quantitative real-time PCR, 1 μ g of total RNA was reverse-transcribed in 50 μ L of TaqMan reverse transcription reagents (Applied Biosystems) using random hexamer primers. cDNA (2 μ L) and the real-time PCR primers (1 μ M) were used in a final 20 μ L qPCR reaction with a SYBR-green master mix (Applied Biosystems). The real-time primers were purchased from Sigma-Aldrich. The sequences of the various primers are shown in Supplementary Tables 2 and 3. Real-time qPCR was performed in an ABI-Prism7900 sequence detection system. Data were analyzed by the comparative Ct method; the expression of the target genes was normalized to *Gapdh* as an endogenous control and is displayed as fold-change relative to a common reference value, which had the highest relative Ct (Δ Ct) and whose expression level was designated as 1. Data are representative of tumor tissues or normal controls kidneys isolated from three to five different mice for each genotype.

Statistical Analysis

Data from different groups were compared by using the Mann–Whitney U test. A difference was considered significant if the *P* value was less than .05. Data are presented as mean \pm standard error of the mean (SEM).

Results

Wt1-Igf2 Mutant Mice Developed Large Tumors But Not Controls

Wt1-Igf2 mutant mice developed tumors with very high frequency (100%) and with splenomegaly compared to littermate controls. Palpable tumors were noted in all mutant mice, but not in controls, beginning at about 10 weeks of age (Figure 1, A and B). Mutant and control mice were euthanized at around 3 months of age and their tumors and kidneys collected and processed for further analysis. Tumor bearing kidneys were typically 10-fold larger in size and weight than littermate control kidneys (Figure 1B). Most of the tumor bearing mice (83% of the mice, 15 out 18 mice) also showed splenomegaly (Figure 1 B&C) with almost 5 fold increases in spleen size.

Up-Regulation of COX2 in the Tumor Microenvironment

The IHC examination of COX-2 in mouse tumor tissues (Figure 2, A and B) was consistent with our findings in human tumors as reported previously [3]. All mouse tumors showed robust expression of COX-2 (Figure 2B) compared to control kidneys (Figure 2A). In addition, RPPA analysis of mouse mesenchymal cells (M15) in which WT1 was knocked down revealed up regulation of COX-2 (Figure 2E). Both of these observations suggest that the COX-2 pathway may be activated when the *Wt1* gene is ablated.

Expression of Downstream Targets of Cox2 Pathway Components in the Tumor Microenvironment

To further demonstrate the activation of this pathway, the downstream targets of the COX-2 pathway were also evaluated by IHC. The results showed that HIF-1 α was overexpressed in mouse tumors in a manner spatially similar to COX-2 (Figure 3, A–C) and similar to that in human tumors (Figure 3, D–F). HIF-1 α also may be activated through the MAPK pathway; our IHC analysis showed the induced expression of MAPK (p-ERK1/2) in mouse tumors stroma (Figure 3, G–I), which was consistent with that noted in human tumors (Figure 3, J–L).

Increased Infiltration of Immunosuppressive Immune Cells in Tumor Microenvironment

Further characterization of the microenvironment of mouse tumors for various inflammatory cells by flow cytometry revealed significantly greater infiltration of immunosuppressive pDCs in tumors than in controls (Figure 4, A and B). The infiltration of pDCs into the tumor microenvironment may have been the mechanism underlying up regulation of the immunosuppressive enzyme indolamine 2, 3-dioxygenase (IDO), which suppresses the function of other immune cells (Figure 4, C and D).

In general, pDCs recruit other immunosuppressive immune cells, the Tregs (CD4⁺CD25⁺FoxP3⁺). Our analysis showed significantly greater infiltration of Treg cells in tumors than in control kidneys (Figure 5, A–C). Furthermore, expression of Fox-3, an important regulator of Tregs, was increased in tumor cells compared to littermate control kidneys, as shown by immunofluorescence imaging (Figure 5D). This comprehensive analysis of WT and adjacent normal kidneys by various methodologies strongly suggests the immunosuppressive effect of the tumor microenvironment in WT tumorigenesis. Though there is a significant difference in size and weights of spleens of control mice and tumor bearing mice, interestingly there was no significant change in the immune cell composition of spleens were observed. The flow cytometric analysis data is shown in supplementary Figs. 1 and 2.

Immunosuppressive Cytokines are Secreted in the Tumor Microenvironment

Infiltration of immunosuppressive inflammatory immune cells in the tumor microenvironment would be expected to induce immunosuppressive chemokines (or vice versa), so we investigated the expression of various inflammatory chemokines and cytokines in the tumor microenvironment with specific primers (Supplementary Table 2) by qPCR. As we anticipated, expression of immunosuppressive cytokines

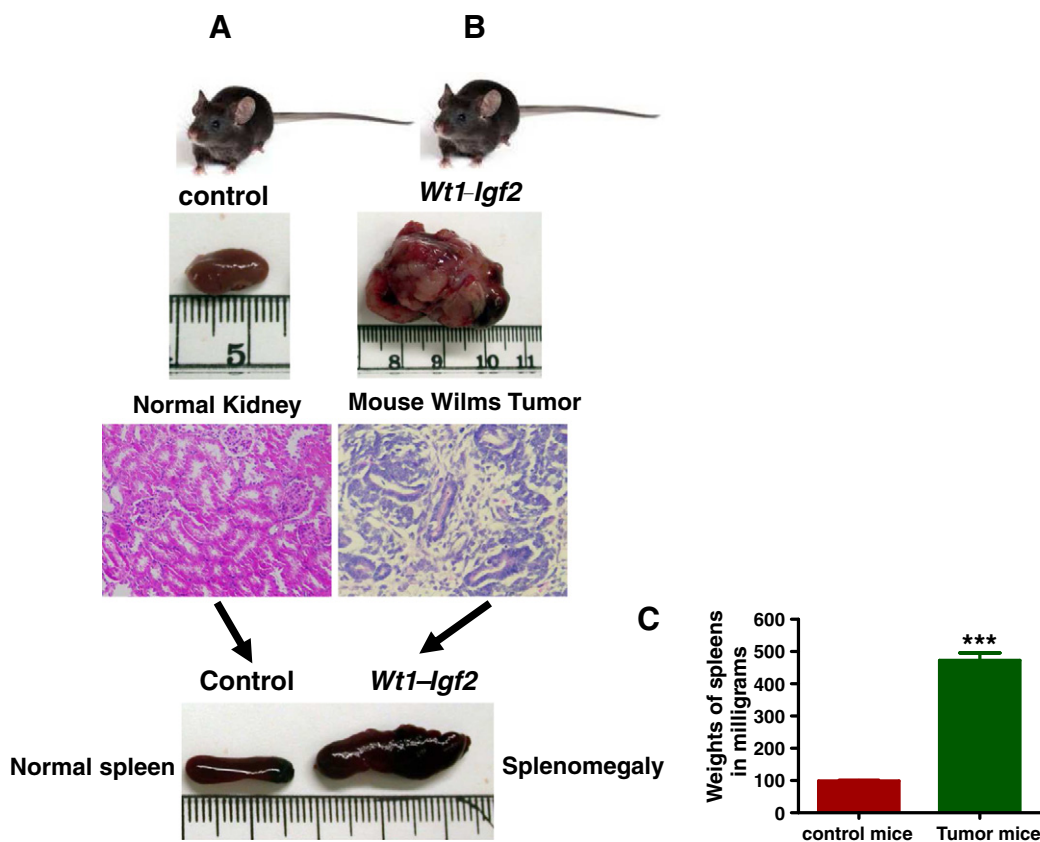


Figure 1. *Wt1-Igf2* mice developed tumors at 3–4 months age. *Wt1-Igf2* mutant mice developed tumors with very high frequency (100%) compared to littermate controls. Palpable tumors were noted in all mutant mice (1B), but not in controls (1A), beginning at about 10 weeks of age. Tumor bearing kidneys were typically 10-fold larger in size and weight (1B) than littermate control kidneys (1A). The mutant mice showed the tumor histology (1B) with typical blastema, epithelia and stroma whereas control kidneys showed normal histology (1A) with H&E staining. Most of the mutant mice also showed splenomegaly (1B). Spleens of the tumor bearing mice were significantly larger than their litter mate controls by size (1B) and weight (1C).

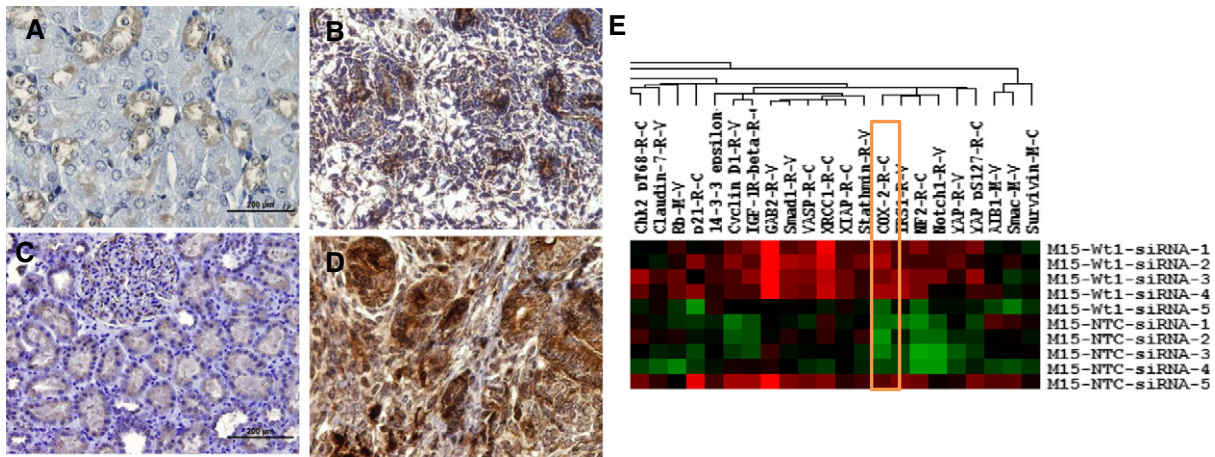


Figure 2. Cox-2 was overexpressed in tumor tissues and upregulated in M15 cell line after Wt1 knockdown. Immunohistochemical analysis of control kidneys from mouse (2A) and tumors (2B) showed robust expression of inflammatory marker COX2 with minimal expression in tubules of the control kidneys (2A). This COX2 expression was similar to human normal kidneys (2C) and tumors (2D) respectively. RPPA analysis of mouse mesenchymal cells (M15) in which WT1 was knocked down revealed up regulation of COX-2 (2E) (marked with orange rectangular box). The expression of these genes in each compartment is visualized as heat map. Red indicates up-regulated genes and green indicates down-regulated genes.

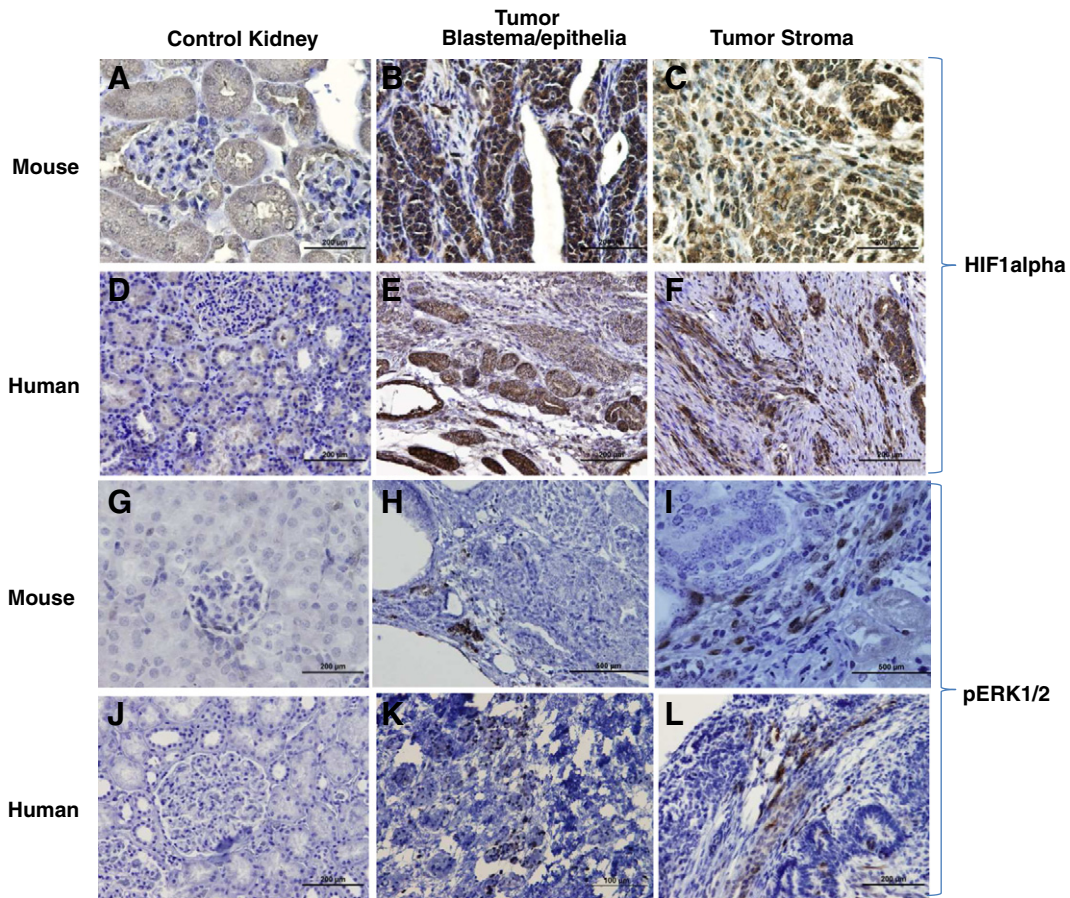


Figure 3. HIF 1 alpha and pERK1/2 expression in mouse and human tumors. To demonstrate the activation of COX2 pathway, its downstream targets HIF-1 α and MAPK (p-ERK1/2) were evaluated by IHC. HIF-1 α was overexpressed in mouse tumors (3B and 3C) compared to control kidneys (3A) and similar to human tumors (3E and 3F) and normal kidneys (3D) respectively. Similarly, MAPK (p-ERK1/2) expression in mouse tumors (Figs. 3G-I) was consistent with the human tumors (Figs. 3J-L).

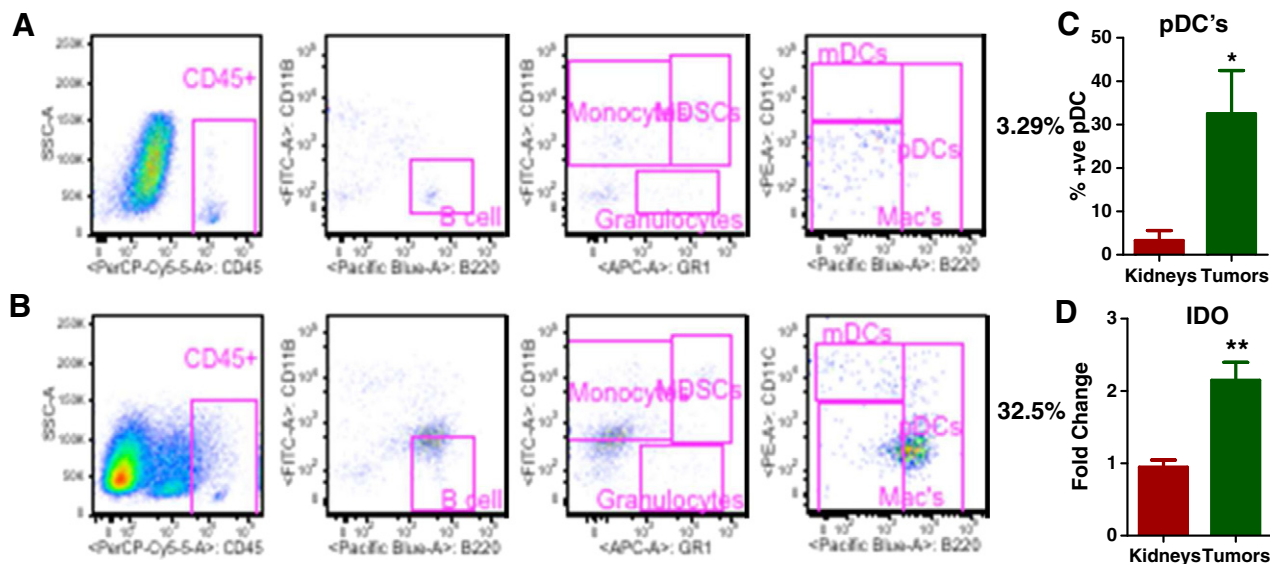


Figure 4. Mouse tumors were infiltrated with immunosuppressive plasmacytoid dendritic cells (pDCs). Flow cytometry analysis of littermate control kidneys (4A) and mouse tumors (4B) showed significantly greater infiltration of immunosuppressive pDCs in tumors (4B) than its littermate control kidneys (4A). To elucidate the underlying mechanism of pDCs infiltration, an immunosuppressive enzyme indolamine 2, 3-dioxygenase (IDO) was analyzed by Q-PCR with IDO specific primers, which was shown to be upregulated in the tumors compared to controls (4D). All data are shown as mean \pm SEM, $n = 5-6$ mice/group ($*** P < .001$, $** P < .01$).

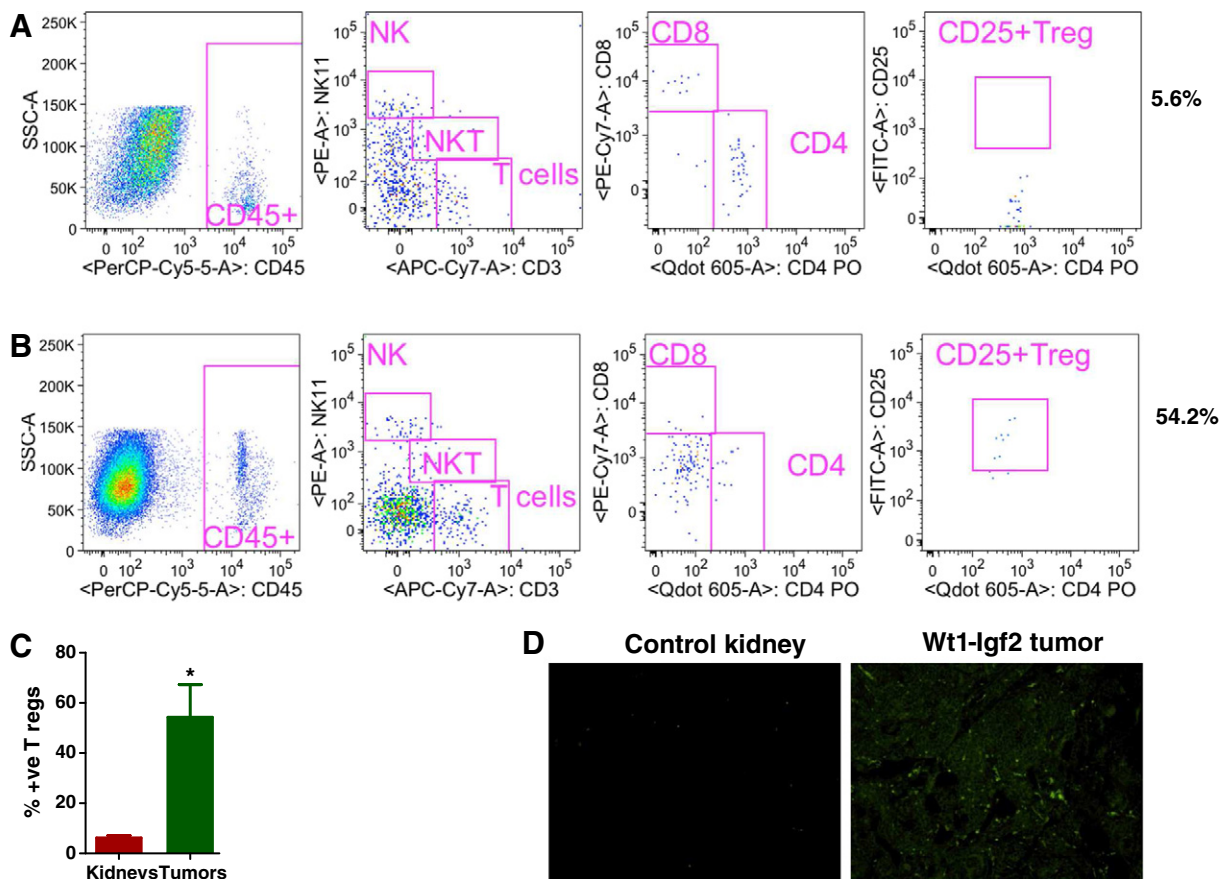


Figure 5. Increased infiltration of immunosuppressive T regulatory cells in mouse tumors. Analysis of tumors by flow cytometry showed significantly greater infiltration of Treg cells in tumors than in control kidneys (5A-C). Expression of Foxp3, an important regulator of Tregs, was increased in tumor cells (Figure 5D) compared with control kidneys by immunofluorescence analysis. All data are shown as mean \pm SEM, $n = 5-6$ mice/group ($*** P < .001$, $** P < .01$).

such as interleukin-10 (IL-10), transforming growth factor beta (TGF- β), and tumor necrosis factor alpha (TNF- α) was upregulated (Figure 6, A–C). However, the expression of various other proinflammatory cytokines was not changed in the tumor microenvironment, such as IL-1 β , IL-4, and IL-6 (Figure 6, D–F). Other cytokines such as IL-8, IL-12, and IL-23 were also expressed to significantly greater levels in the tumor tissues than in the control kidneys.

Chemotactic Chemokines Responsible for Immunosuppressive Inflammatory Cell Infiltration are Expressed in the Tumor Microenvironment

To further elucidate the mechanisms involved in the recruitment of the immunosuppressive immune cells in the tumor microenvironment, we analyzed various chemotactic chemokines and their receptors specific for these immune cells with chemokine specific primers (Supplementary Table 3). Expression of chemotactic chemokines such as CCL3, CCL4, and

CCL5, specific for CCR5 chemokine receptor (Figure 7, A–C); CCL17 and CCL22, specific for CCR4 chemokine receptor (Figure 7, D and E); and CCL20, specific for CCR6 receptor (Figure 7F), which are known to be responsible for Treg cell recruitment, were increased in the tumors. The pDC-specific chemokine CXCL12, a ligand for CXCR4, was also up-regulated in the tumors (Figure 7G). These data suggest that infiltration of Tregs and pDCs into the tumor microenvironment was dependent most specifically on CCR5 and CXCR4, respectively (Figure 9).

Role of COX2 in inflammatory immune cell recruitment

COX-2 has been implicated in Treg trafficking and production. It also is known to activate p-STAT3, and we speculated that this may be a mechanism underlying the Treg induction and infiltration and thus creation of the immunosuppressive tumor microenvironment we observed in WT. To test this, we analyzed p-STAT3 expression in mouse tumors (Figure 8, A and B) by IHC and the human tumors by IHC (Figure 8, C and D) and RPPA (Figure 8E).

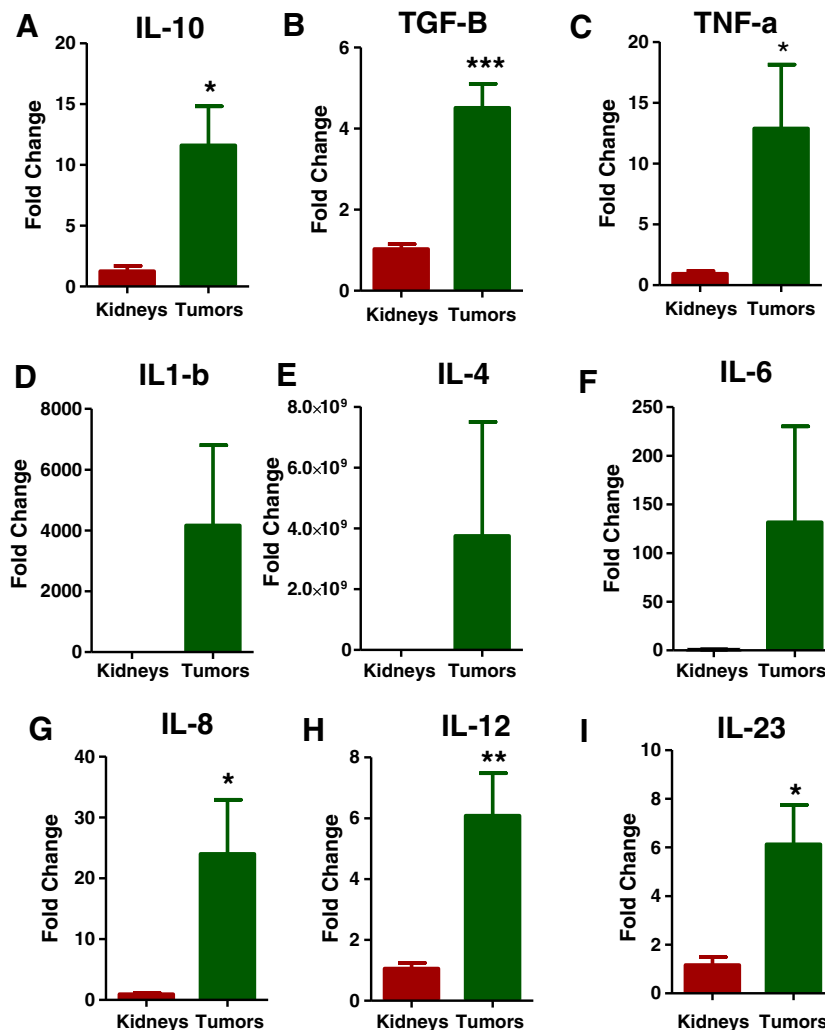


Figure 6. Tregs may induce the secretion of immune suppressive cytokines. Q-PCR analysis of immunosuppressive cytokines such as interleukin-10 (IL-10) (6A), transforming growth factor beta (TGF- β) (6B), and tumor necrosis factor alpha (TNF- α) (6C) were increased in tumors compared to controls. Other proinflammatory cytokines IL-1 β , IL-4, and IL-6 (Figs. 6D–F) were not significantly upregulated, but IL-8 (6G), IL-12(6H), and IL-23 (6I) were expressed at significantly greater levels in the tumor tissues than in the control kidneys. All data are shown as mean \pm SEM, n = 3–4 mice/group (***) $P < .001$, ** $P < .01$).

The more abundant expression of p-STAT3 in both mouse and human tumors than in control tissues provides evidence for a role of COX-2 in promoting the immunosuppressive microenvironment.

More pronounced Th2 and treg induced cytokine response in the tumor microenvironment than Th1 response

T-helper cell (Th) response analysis in the mouse tumors showed that the Th2 response was greater than the Th1 and Th17 responses (Figure 10, A and B). The qPCR analysis showed that the inflammatory cytokines responsible for the Th2 response (Figure 6, D–I) and the Treg response (Figure 6, A–C) were also up-regulated. This suggests that Treg-induced cytokines as well as Th2 induced cytokines may be more important than Th1 response in creating the immunosuppressive microenvironment.

Discussion

It is well known that dysregulated or altered signaling pathways are the major cause of cancer development, including WT. COX-2, an isoform of the enzyme cyclooxygenase, is induced by various cytokines, mitogens, and growth factors [8]. COX-2 has been reported as a therapeutic target in various tumors and tumor models [9–11] because of its expression in tumors as well as premalignant lesions. Since COX-2 possesses antiapoptotic [12,13] and proangiogenic properties [14,15], its induction in the tumor microenvironment or precancerous cells has a potential role in promoting tumor growth.

The study presented here found that COX-2 was overexpressed in all the mouse tumors and its expression was similar to that in human WTs. Moreover, COX-2 expression was localized to tumor stroma and other components of tumor, as normal kidney samples showed

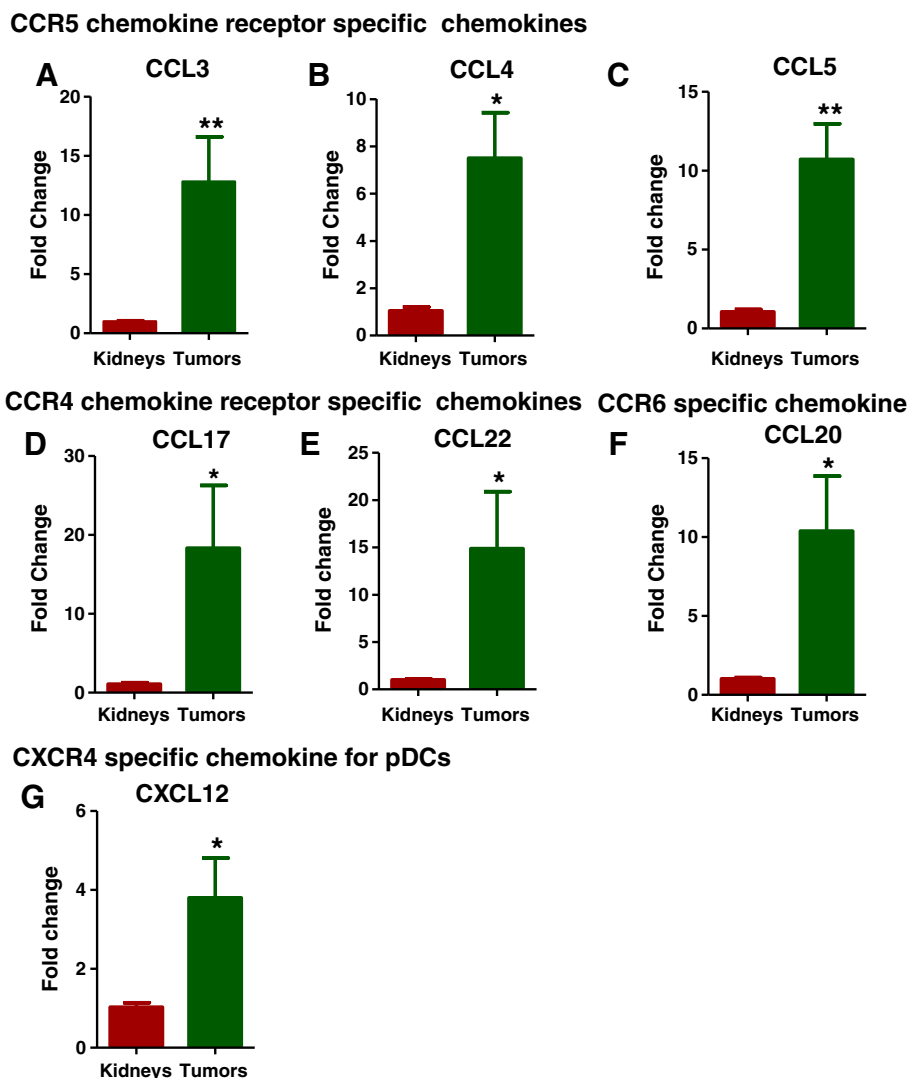


Figure 7. Chemokines specific for Tregs and p-DCs recruitment were upregulated. The chemotactic chemokines specific for pDCs and Treg recruitment were analyzed by Q-PCR. Expression of chemotactic chemokines such as CCL3, CCL4, and CCL5, specific for CCR5 chemokine receptor (7A-C); CCL17 and CCL22, specific for CCR4 chemokine receptor (7D and 7E); and CCL20, specific for CCR6 receptor (7F), which are known to be responsible for Treg cell recruitment, were increased in the tumors. The pDC-specific chemokine CXCL12, a ligand for CXCR4, was also upregulated in the tumors (7G). All data are shown as mean \pm SEM, n = 3–4 mice/group (***) $P < .001$, ** $P < .01$.

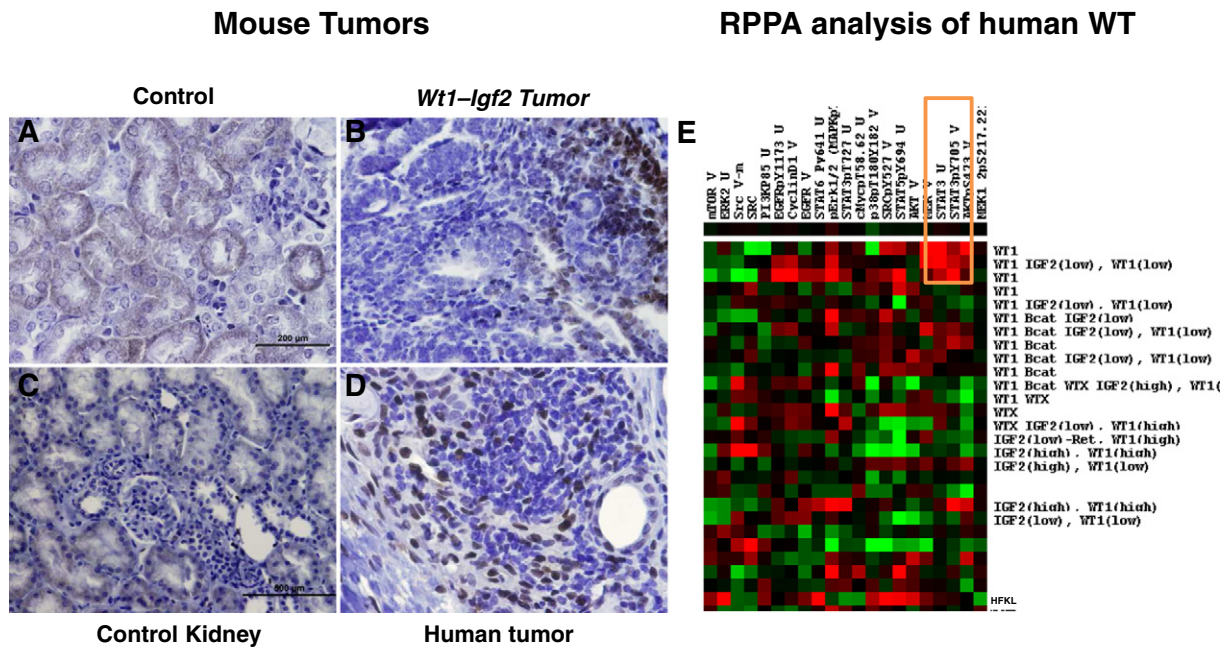


Figure 8. Increased p-Stat3 expression in mouse and human tumors. We performed immunohistochemical analysis of p-STAT3 expression in mouse control kidneys (8A), mutant tumors (8B), human control kidney (8C) and human tumors (8D). Increased expression of p-STAT3 in tumors than in control kidneys was observed, and RPPA (8E) analysis of human tumors also showed upregulated expression of STAT3 (marked with orange rectangular box). The expression of these genes in each compartment is visualized as a heat map. Red indicates upregulated genes and green indicates down-regulated genes.

only weak to moderate staining in the cytoplasm of some tubular epithelial cells and very weak or no staining in renal interstitial cells or glomeruli, which is normal. These observations point toward activation of the COX-2 pathway in WT pathogenesis. Various mechanisms may underlie, individually or in combination, the upregulation and activation of COX-2. First, the infiltrating immune cells themselves could be overexpressing COX-2. Second, tumor fibroblasts could be generating COX-2 in the tumor microenvironment. Third, COX-2 expression in these tumors may be induced by the fetal mitogen IGF2 via the Ras/Raf/MEK/ERK pathway, which has been reported in human keratinocytes [16].

To further confirm the activation of the COX-2 pathway in the tumor microenvironment, we analyzed the expression of downstream targets of the pathway. Both HIF-1 α and p-ERK1/2, which are downstream targets of the COX-2 pathway, were overexpressed in the

mouse tumors, a finding consistent with our previous report that both were upregulated in human WTs [3]. This overexpression of p-ERK1/2, which may be due to increased IGF2 expression, suggests a role of ERK signaling in WT development. The robust expression of COX-2 and pERK1/2 in these tumors further suggests that one consequence of IGF2 overexpression in WT is COX-2 up regulation and promotion of an inflammatory microenvironment, which may be mediated by enhanced ERK signaling.

In tumor analysis by flow cytometry, the tumor-associated pDCs (CD11c⁺/B220⁺) were significantly upregulated in the tumor compared to control kidneys. These pDCs induce IL-10-producing Tregs and secretion of various immunosuppressive soluble factors, proinflammatory chemokines, and cytokines, thereby leading to immunosuppression-mediated tumor progression. In a second panel of immune cell analysis done to verify the infiltration of IL-10-

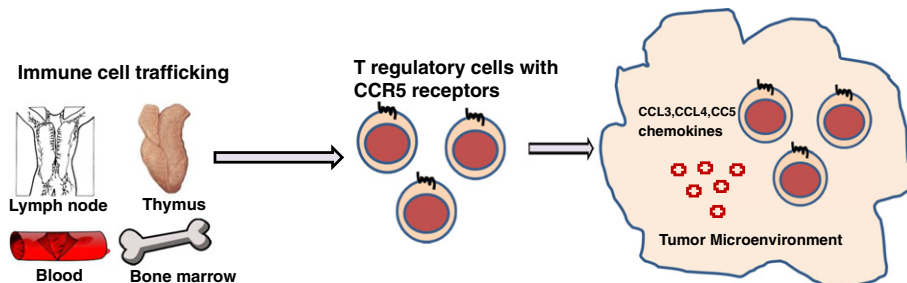


Figure 9. Tregs are recruited to the tumor microenvironment by chemokine and chemokine receptor signaling in a CCR5 dependent manner.

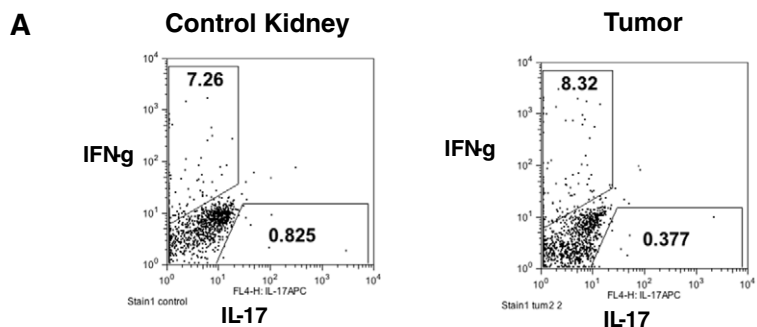
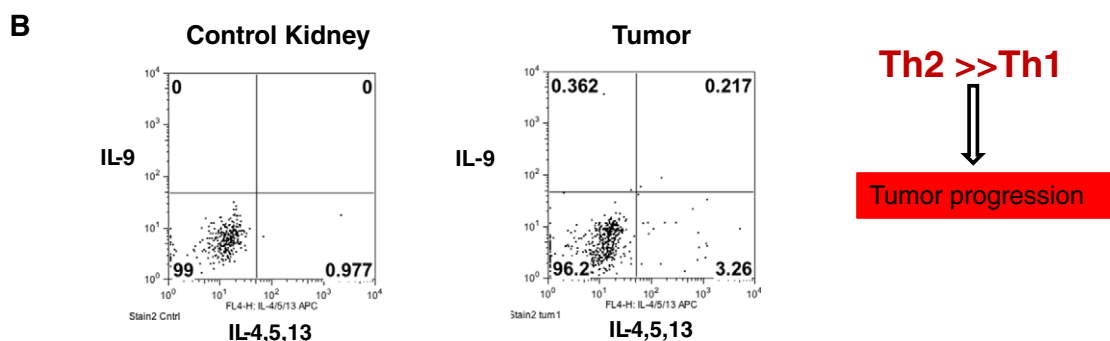
Th1 induced cytokine response**Th2 induced cytokine response**

Figure 10. More pronounced Th2 induced cytokine response than Th1 response in the tumors. T-helper cell (Th) response analysis by flow cytometry in the mouse tumors showed that the Th2 induced cytokine response was greater than the Th1 and Th17 responses (Figs. 10A and B). The qPCR analysis showed that the inflammatory cytokines responsible for the Th2 response (Figs. 6D-I) and the Treg response to a maximum extent (Figs. 6A-C) were also upregulated. All data are shown as mean \pm SEM, $n = 5-6$ mice/group (** $P < .001$, ** $P < .01$).

producing Tregs, we were able to see increased infiltration of inflammatory $CD4^+/CD25^+/Foxp3^+$ Treg cells. As we anticipated, immunosuppressive cytokines such as IL-10, TGF- β , and TNF- α also were upregulated, as were various other proinflammatory cytokines such as IL-8, IL-12, and IL-23, in the tumor microenvironment. This up regulation of proinflammatory factors may have been due to the increased immune cell infiltration and would have further aggravated tumor growth. Expression of another important immunosuppressive soluble inflammatory factor produced by pDCs, IDO [17], was also increased in the tumors. The intracellular enzyme IDO and increased infiltration of pDCs in the tumor microenvironment has been reported in various cancers [18–20]. It has been reported that pDC infiltration into solid tumors reduce the induction of T-cell activation [21] or infiltration of IL-10–producing $CD4^+/CD25^+$ Tregs that inhibit antitumor immunity [22,23]. These tumor-associated pDCs are defective in IFN- γ production but instead secrete immunosuppressive soluble factors responsible for tumor progression [24].

It is speculated that trafficking of various inflammatory cells into the tumor site occurs through selective migration and an accumulative retention system or a chemotactic response. Current data suggest that the capacity of Treg cells and pDCs to migrate into the tumor site is controlled by the chemokine/chemokine receptor system. Interestingly, CCR4, CCR5, and CCR6 receptor-specific chemokines were upregulated in the tumors compared to control

kidneys. It has been reported that Tregs express CCR4, CCR5, and CCR6 chemokine receptors [25–27]. The chemotactic chemokines such as CCL22, specific for the CCR4 receptor; CCL3, CCL4, and CCL5, specific for the CCR5 chemokine receptor; and CCR6 receptor–specific chemokine CCL20 secreted in the tumors may have been responsible for the selective Treg recruitment observed in the tumor microenvironment (Figure 9), which results in reduced tumor-specific immunity [27]. Certainly, the expression pattern of various chemokines in the tumor microenvironment suggests an immunosuppressive milieu. We also observed increased expression of another chemokine, CXCL12, a ligand for CXCR4 that is known to be expressed by pDCs [28]. In this tumor model, tumor-derived CXCL12 may contribute to the trafficking and accumulation of pDCs in the tumor. These pDCs are ineffective in stimulation of immune responses but can induce T cell tolerance, possibly through up regulation of immunosuppressive IDO [29]. In other cancers, this IDO accumulation was attributed to CXCL-12 secreted by tumor cells [21,30]. In this model of WT, the CXCL12/CXCR4 axis may be responsible for trafficking of pDCs into the tumor microenvironment, where they produce IDO.

It has been reported that COX-2 is responsible for an immunosuppressive network and induces Treg cell–specific transcription factor FoxP3 to increase Treg cell activity [31]. Sharma et al. showed that inhibition of COX-2 reduced Treg cell activity as well as

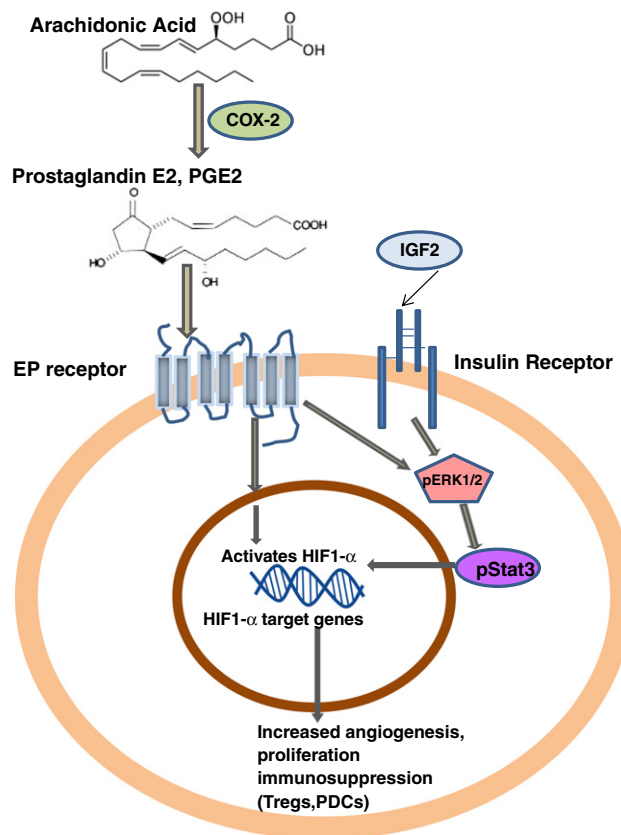


Figure 11. Mechanism of action of COX-2 in creating immunosuppressive tumor microenvironment. The upregulated COX-2 expression creates an inflammatory microenvironment in WT which may be mediated by enhanced p-ERK signaling leading to activation of HIF-1 α target genes via p-STAT3. In another way, COX-2 can also activate the expression of HIF-1 α through its enzymatic product prostaglandin E2. HIF-1 α can also directly upregulate expression of COX-2 during hypoxia and thus form a feedback loop to continually activate the COX-2 pathway. Hence, it may be assumed that COX-2 affects the inflammation, hyperproliferation, and angiogenesis and immunosuppression (Tregs, PDCs) in WT by IGF2 induced COX-2 mediated p-ERK1/2 pathway.

trafficking and thereby reduced tumor burden [32]. Therefore, COX-2 expression mediates immunosuppression, and its inhibition suppresses Treg cell activity and enhances antitumor immune responses. From these results, we can predict that, in addition to chemokine-mediated chemotaxis, COX-2 also might play a significant role in Treg cell trafficking.

One mechanism for immunosuppression in the tumor microenvironment has been shown to be activation of p-STAT3 and thus induction of Treg cell infiltration [32–35]. Earlier studies clearly pointed to the important roles of COX-2 in p-STAT3 activation [33] and of p-STAT3 in Treg generation [36]. The more abundant expression of p-STAT3 in both mouse and human tumors than in control kidney tissues by both IHC and RPPA analysis in this study may support a role of COX-2 in Treg cell generation and immunosuppression via STAT3 activation.

The homeostasis of the immune system for providing an antitumor response is coordinated to a large extent by cytokines produced by various CD4⁺ T helper cells such as the Th1, Th2, and Th17 lymphocyte subsets. These helper T cells also influence innate immunity by helping to shape the character and magnitude of the inflammatory response. The CD4⁺ Th1 cells produce interferon gamma (IFN- γ) and, with the help of mature DCs, type 1 natural killer T cells, CD8⁺ T cells, and other cells, mount an effective

antitumor response, whereas CD4⁺ Th2 cells, in cooperation with Tregs, myeloid-derived suppressor cells, immature DCs, and other cells, suppress the antitumor response by producing inflammatory and immunosuppressive cytokines such as IL-4, IL-5, IL-6, IL-10, and IL-13, leading to tumor progression.

T-helper cell response analysis in this tumor study showed that the Th2 response in these mouse tumors was greater than the Th1 and Th17 responses. This was validated by the qPCR analysis showing that inflammatory cytokines responsible for Th2 response and Treg response were upregulated. Changes in Th1- or Th2-associated cytokines leading to decreased Th1/Th2 ratios has been reported in various cancers, such as pancreatic cancer [37], lung cancer [38], breast cancer [39], and other cancers [40]. It is evident from the literature [41] that the COX-2 in the tumor microenvironment not only induces Treg production and Treg cell trafficking but also polarizes toward Th2 helper response rather than Th1 response. COX-2 plays an important role in the shift from the Th1 profile to production of cytokines, leading to reduced activation of the antitumor response via Th2 response activation. This ability of COX-2 to suppress the immune response allows tumor cells to escape immunosurveillance, adding to the already myriad roles of the COX-2/PGE2 pathway in tumor development. Together, this evidence indicates that COX-2 may be a primary target in these

tumors for regulating the immune suppression that controls immune cell trafficking by chemotaxis or activation of various immunosuppressive cytokines (Figure 11).

Conclusions

We conclude that the COX-2 pathway is a potential beneficial target for the treatment of WT. It may be most effective as an adjuvant therapy together with other inhibitors because of the many advantages of such a regimen over irradiation, conventional cytotoxic treatment, or other novel agents used to treat WT. The youngest children with WT are particularly at risk for irreversible adverse effects from irradiation. Since ionizing radiation induces COX-2 expression, the concomitant use of agents targeting the production of prostanoids may be beneficial for patients through both improved antitumor efficacy and putative limitation of adverse long-term neurological side effects. Our current study provides a good rationale for initiating animal studies to confirm the efficacy of COX-2 inhibitors in decreasing tumor cell growth in vivo.

Supplementary data to this article can be found online at <http://dx.doi.org/10.1016/j.neo.2016.07.009>.

Conflicts of Interest

None.

Acknowledgements

The expert scientific help of Vicki Huff, Professor, Department Genetics, MD Anderson Cancer Center, Houston, TX, USA, is greatly appreciated. This work was supported by U.S. National Institutes of Health grants CA34936 and DK069599 and by State of Texas CPRIT grants RP110324 and RP100329.

References

- Davidoff AM (2012). Wilms tumor. *Adv Pediatr Infect Dis* **59**, 247–267.
- Zirn B, Hartmann O, Samans B, Krause M, Wittmann S, Mertens F, Graf N, Eilers M, and Gessler M (2006). Expression profiling of Wilms tumors reveals new candidate genes for different clinical parameters. *Int J Cancer* **118**, 1954–1962.
- Maturu P, Overwijk WW, Hicks J, Ekmekcioglu S, Grimm EA, and Huff V (2014). Characterization of the inflammatory microenvironment and identification of potential therapeutic targets in Wilms tumors. *Transl Oncol* **7**, 484–492.
- Hu Q, Gao F, Tian W, Ruteshouser EC, Wang Y, Lazar A, Stewart J, Strong LC, Behringer RR, and Huff V (2011). Wt1 ablation and Igf2 upregulation in mice result in Wilms tumors with elevated ERK1/2 phosphorylation. *J Clin Invest* **121**, 174–183.
- Hendry CE, Vanslambrouck JM, Ineson J, Suhaimi N, Takasato M, Rae F, and Little MH (2013). Direct transcriptional reprogramming of adult cells to embryonic nephron progenitors. *J Am Soc Nephrol* **24**, 1424–1434.
- Tibes R, Qiu Y, Lu Y, Hennessy B, Andreeff M, Mills GB, and Kornblau SM (2006). Reverse phase protein array: validation of a novel proteomic technology and utility for analysis of primary leukemia specimens and hematopoietic stem cells. *Mol Cancer Ther* **5**, 2512–2521.
- Eisen MB, Spellman PT, Brown PO, and Botstein D (1998). Cluster analysis and display of genome-wide expression patterns. *Proc Natl Acad Sci U S A* **95**, 14863–14868.
- Bodey B, Siegel SE, and Kaiser HE (2006). Cyclooxygenase-2 (COX-2) overexpression in childhood brain tumors. *In Vivo* **20**, 519–525.
- Baryawno N, Sveinbjornsson B, Eksborg S, Orrego A, Segerstrom L, Oqvist CO, Holm S, Gustavsson B, Kagedal B, and Kogner P, et al (2008). Tumor-growth-promoting cyclooxygenase-2 prostaglandin E2 pathway provides medulloblastoma therapeutic targets. *Neuro Oncol* **10**, 661–674.
- Zhao Q, Wang C, Zhu J, Wang L, Dong S, Zhang G, and Tian J (2011). RNAi-mediated knockdown of cyclooxygenase2 inhibits the growth, invasion and migration of SaOS2 human osteosarcoma cells: a case control study. *J Exp Clin Cancer Res* **30**, 26.
- Parashar B, Latha Shankar S, O'Guin K, Butler J, Vikram B, and Shafti-Zagardo B (2005). Inhibition of human neuroblastoma cell growth by CAY10404, a highly selective Cox-2 inhibitor. *J Neurooncol* **71**, 141–148.
- Lin C, Crawford DR, Lin S, Hwang J, Sebuyira A, Meng R, Westfall JE, Tang HY, Lin S, and Yu PY, et al (2011). Inducible COX-2-dependent apoptosis in human ovarian cancer cells. *Carcinogenesis* **32**, 19–26.
- Kuper C, Bartels H, Beck FX, and Neuhof W (2011). Cyclooxygenase-2-dependent phosphorylation of the pro-apoptotic protein Bad inhibits tonicity-induced apoptosis in renal medullary cells. *Kidney Int* **80**, 938–945.
- Finetti F, Solito R, Morbidelli L, Giachetti A, Ziche M, and Donnini S (2008). Prostaglandin E2 regulates angiogenesis via activation of fibroblast growth factor receptor-1. *J Biol Chem* **283**, 2139–2146.
- Lyons TR, Borges VF, Betts CB, Guo Q, Kapoor P, Martinson HA, Jindal S, and Schedin P (2014). Cyclooxygenase-2-dependent lymphangiogenesis promotes nodal metastasis of postpartum breast cancer. *J Clin Invest* **124**, 3901–3912.
- Tjiu JW, Chen JS, Shun CT, Lin SJ, Liao YH, Chu CY, Tsai TF, Chiu HC, Dai YS, and Inoue H, et al (2009). Tumor-associated macrophage-induced invasion and angiogenesis of human basal cell carcinoma cells by cyclooxygenase-2 induction. *J Invest Dermatol* **129**, 1016–1025.
- Poormasjedi-Meibod MS, Jalili RB, Hosseini-Tabatabaei A, Hartwell R, and Ghahary A (2013). Immuno-regulatory function of indoleamine 2, 3 dioxygenase through modulation of innate immune responses. *PLoS One* **8**, e71044.
- Chauhan D, Singh AV, Brahmandam M, Carrasco R, Bandi M, Hideshima T, Bianchi G, Podar K, Tai YT, and Mitsiades C, et al (2009). Functional interaction of plasmacytoid dendritic cells with multiple myeloma cells: a therapeutic target. *Cancer Cell* **16**, 309–323.
- Charles J, Chaperot L, Salameire D, Di Domizio J, Asford C, Gressin R, Jacob MC, Richard MJ, Beani JC, and Plumas J, et al (2010). Plasmacytoid dendritic cells and dermatological disorders: focus on their role in autoimmunity and cancer. *Eur J Dermatol* **20**, 16–23.
- Le Mercier I, Poujol D, Sanlaville A, Sisirak V, Gobert M, Durand I, Dubois B, Treilleux I, Marvel J, and Vlach J, et al (2013). Tumor promotion by intratumoral plasmacytoid dendritic cells is reversed by TLR7 ligand treatment. *Cancer Res* **73**, 4629–4640.
- Vermi W, Bonecchi R, Facchetti F, Bianchi D, Sozzani S, Festa S, Berenzi A, Cella M, and Colonna M (2003). Recruitment of immature plasmacytoid dendritic cells (plasmacytoid monocytes) and myeloid dendritic cells in primary cutaneous melanomas. *J Pathol* **200**, 255–268.
- Schettini J and Mukherjee P (2008). Physiological role of plasmacytoid dendritic cells and their potential use in cancer immunity. *Clin Dev Immunol* **2008**, 106321.
- Sharma MD, Baban B, Chandler P, Hou DY, Singh N, Yagita H, Azuma M, Blazar BR, Mellor AL, and Munn DH (2007). Plasmacytoid dendritic cells from mouse tumor-draining lymph nodes directly activate mature Tregs via indoleamine 2,3-dioxygenase. *J Clin Invest* **117**, 2570–2582.
- Fallarino F, Gizzi S, Mosci P, Grohmann U, and Puccetti P (2007). Tryptophan catabolism in IDO+ plasmacytoid dendritic cells. *Curr Drug Metab* **8**, 209–216.
- Lim HW, Lee J, Hillsamer P, and Kim CH (2008). Human Th17 cells share major trafficking receptors with both polarized effector T cells and FOXP3+ regulatory T cells. *J Immunol* **180**, 122–129.
- Tan MC, Goedegebuure PS, Belt BA, Flaherty B, Sankpal N, Gillanders WE, Eberlein TJ, Hsieh CS, and Linehan DC (2009). Disruption of CCR5-dependent homing of regulatory T cells inhibits tumor growth in a murine model of pancreatic cancer. *J Immunol* **182**, 1746–1755.
- Mukaida N, Sasaki S, and Baba T (2014). Chemokines in cancer development and progression and their potential as targeting molecules for cancer treatment. *Mediators Inflamm* **2014**, 170381.
- Obermajer N, Muthuswamy R, Odunsi K, Edwards RP, and Kalinski P (2011). PGE(2)-induced CXCL12 production and CXCR4 expression controls the accumulation of human MDSCs in ovarian cancer environment. *Cancer Res* **71**, 7463–7470.
- Rabinovich GA, Gabrilovich D, and Sotomayor EM (2007). Immunosuppressive strategies that are mediated by tumor cells. *Annu Rev Immunol* **25**, 267–296.
- Watts NL (2013). Cancer Immunotherapy: Paradigms, Practice and Promise. *Ann Pharmacother*.
- Ha TY (2009). The role of regulatory T cells in cancer. *Immune Netw* **9**, 209–235.
- Sharma S, Yang SC, Zhu L, Reckamp K, Gardner B, Baratelli F, Huang M, Batra RK, and Dubinett SM (2005). Tumor cyclooxygenase-2/prostaglandin E2-dependent promotion of FOXP3 expression and CD4+ CD25+ T regulatory cell activities in lung cancer. *Cancer Res* **65**, 5211–5220.

- [33] Dalwadi H, Krysan K, Heuze-Vourc'h N, Dohadwala M, Elashoff D, Sharma S, Cacalano N, Lichtenstein A, and Dubinett S (2005). Cyclooxygenase-2-dependent activation of signal transducer and activator of transcription 3 by interleukin-6 in non-small cell lung cancer. *Clin Cancer Res* **11**, 7674–7682.
- [34] Yuan XL, Chen L, Li MX, Dong P, Xue J, Wang J, Zhang TT, Wang XA, Zhang FM, and Ge HL, et al (2010). Elevated expression of Foxp3 in tumor-infiltrating Treg cells suppresses T-cell proliferation and contributes to gastric cancer progression in a COX-2-dependent manner. *Clin Immunol* **134**, 277–288.
- [35] Shimizu K, Nakata M, Hiram Y, Yukawa T, Maeda A, and Tanemoto K (2010). Tumor-infiltrating Foxp3+ regulatory T cells are correlated with cyclooxygenase-2 expression and are associated with recurrence in resected non-small cell lung cancer. *J Thorac Oncol* **5**, 585–590.
- [36] Pallandre JR, Brillard E, Crehange G, Radlovic A, Remy-Martin JP, Saas P, Rohrlich PS, Pivot X, Ling X, and Tiberghien P, et al (2007). Role of STAT3 in CD4 + CD25 + FOXP3+ regulatory lymphocyte generation: implications in graft-versus-host disease and antitumor immunity. *J Immunol* **179**, 7593–7604.
- [37] De Monte L, Reni M, Tassi E, Clavenna D, Papa I, Recalde H, Braga M, Di Carlo V, Dogliani C, and Protti MP (2011). Intratumor T helper type 2 cell infiltrate correlates with cancer-associated fibroblast thymic stromal lymphopoietin production and reduced survival in pancreatic cancer. *J Exp Med* **208**, 469–478.
- [38] Chen YM, Yang WK, Ting CC, Tsai WY, Yang DM, Whang-Peng J, and Perng RP (1997). Cross regulation by IL-10 and IL-2/IL-12 of the helper T cells and the cytolytic activity of lymphocytes from malignant effusions of lung cancer patients. *Chest* **112**, 960–966.
- [39] Rosen HR, Ausch C, Reinerova M, Zaspin E, Renner K, Rosen AC, Schiessel R, and Moroz C (1998). Activated lymphocytes from breast cancer patients express the characteristics of type 2 helper cells—a possible role for breast cancer-associated p43. *Cancer Lett* **127**, 129–134.
- [40] Elsasser-Beile U, Kolble N, Grussenmeyer T, Schultze-Seemann W, Wetterauer U, Gallati H, Schulte Monting J, and von Kleist S (1998). Th1 and Th2 cytokine response patterns in leukocyte cultures of patients with urinary bladder, renal cell and prostate carcinomas. *Tumour Biol* **19**, 470–476.
- [41] Greenhough A, Smartt HJ, Moore AE, Roberts HR, Williams AC, Paraskeva C, and Kaidi A (2009). The COX-2/PGE2 pathway: key roles in the hallmarks of cancer and adaptation to the tumour microenvironment. *Carcinogenesis* **30**, 377–386.